PLASMA SPRAY DEPOSITION OF YTTRIA-STABILIZED ZIRCONIA FOR FUEL CELL APPLICATIONS

C. L. Curtis*, D. T. Gawne* & M. Priestnall†
*Department of Materials Technology, Brunel, the University of West London, Uxbridge, Middlesex, UK
† Cookson Technology Centre, Yarnton, Oxford, UK.

Summary

The electrical conductivity of plasma sprayed yttria-stabilized zirconia decreases with increasing particle size injected into the plasma. The particle size-dependency of conductivity is related to the inadequate flow of particles on impact with the substrate, porosity and the growth of columnar grains across splat boundaries. The results suggest that the interfacial impedance is dominated by the splat boundary configuration and columnar grain boundaries have a secondary effect.

INTRODUCTION.

Yttria-stabilized zirconia is used as an electrolyte in solid oxide fuel cells because it possesses an attractive combination of electrical and mechanical properties. In particular, the conductivity of zirconia can be markedly increased by forming a solid solution in which some of the tetravalent zirconium ions are replaced by trivalent yttrium ions, since this introduces oxygen vacancies charge-compensating defects. Oxygen ions can thus migrate by these vacancies at sufficiently high temperatures (~ 1000°C) giving rise to substantial electrical conductivity.

Thin layers (~ 0.5 mm) of electrolyte have been produced by a variety of processing techniques including tape casting, chemical vapour deposition, physical vapour deposition, slurry coating and plasma spraying [1,2]. This paper concerns an investigation of the effect of feed particle size on the electrical conductivity and microstructure of plasma-sprayed yttria-stabilized zirconia.

EXPERIMENTAL PROCEDURE

The powder samples used in this investigation were prepared from Metco 204 NS, which is 8wt% yttria-stabilized zirconia (YSZ). The powder morphology of this grade is designed for plasma spray deposition. The powder shape and size distribution are given in Figures 1 and 2 respectively. The as-received powder (designated M) was sieved into five size intervals: 20-38 μm (designated A), 38-52 μm (B), 52-75 μm (C), 75-90 μm (D) and 90-110 μm (E). The six classes of powder were deposited on 304 grade stainless steel (18wt% chromium, 10wt% nickel, 0.05wt% carbon) using a Metco MN plasma spray system. Spraying was carried out in air with a stand-off distance of 100 mm to give deposits of 1 mm in thickness.

The electrical conductivity of the samples was measurement by the complex impedance method using a Schlumberger 1260 impedance gain-phase analyzer over the frequency range 100mHz to 10MHz. The experimental apparatus was interfaced with a microcomputer in order to process the data. 5 mm by 5 mm gold contacts were sputtered onto both sides of the samples and connected to 5 mm by 5 mm platinum gauze by silver paint to enable measurements at 380°C. The bulk densities of the deposits were determined at 20°C by the mercury up thrust technique using a Doulton Densimeter.

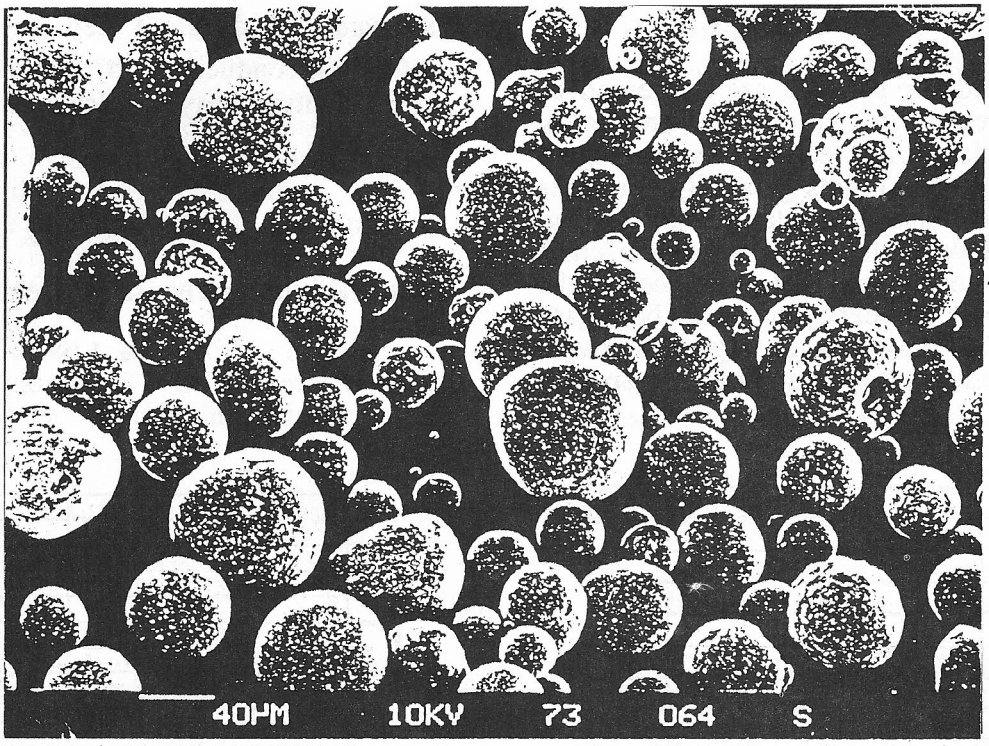

Figure 1. Scanning electron micrograph of YSZ feed powder prior to plasma spraying.

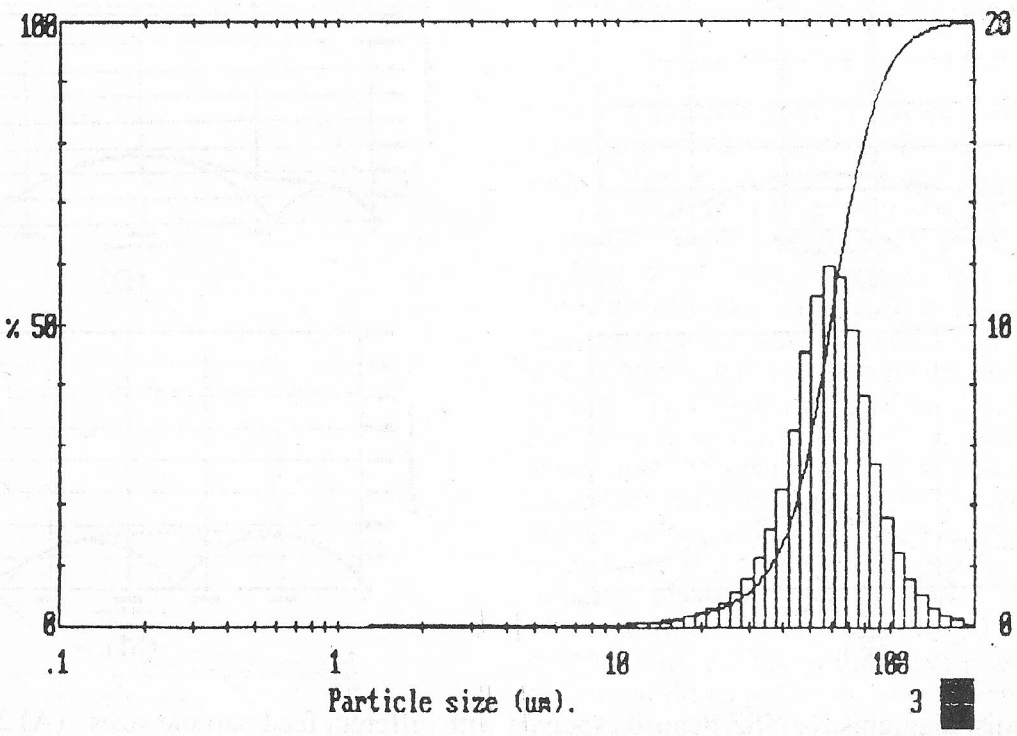

Figure 2. Particle size distribution of the as-received YSZ powder, M.

RESULTS AND DISCUSSION

The conductivity data are expressed as Nyquist diagrams in which the imaginary impedance is plotted the real impedance (Figure 3). The locus of the points generally describes two semicircles: it has been established [1-3] that the semicircle at the higher frequency on the left of the diagram relates to intragrain resistance and the one at the lower frequency to grain boundary resistance. The diagrams in Figure 3 reveal significant differences between samples plasma sprayed with different feed particle sizes. The intragrain conductivity σ_i and grain boundary σ_g conductivity by may be calculated from:

$$\sigma_i = K/R_i \quad (1)$$

$$\sigma_g = K/R_g \quad (2)$$

where K is the cell constant given by:

$$K = L/S \quad (3)$$

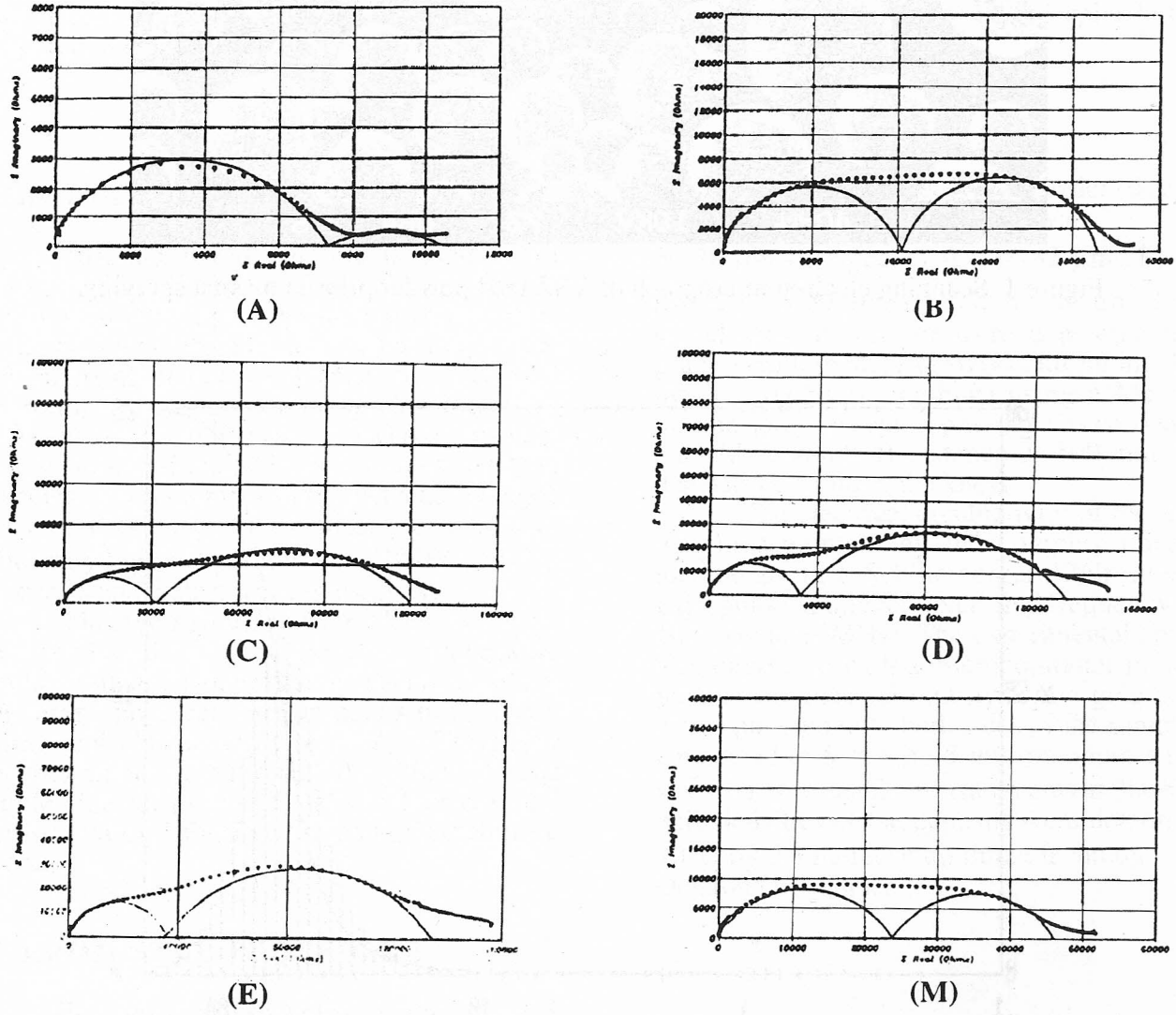

Figure 3. Nyquist diagrams for YSZ deposits sprayed with different feed particle sizes. (A) 20-38 μm, (B) 38-52 μm, (C) 52-75 μm, (D) 75-90 μm, (E) 90-110 μm, (M) 20-110 μm.

where L and S are the sample thickness and cross-sectional area respectively. R_i and R_g are the intercept lengths of the respective semicircle on the real impedance axis. The results are given in Table 1 along with the corresponding density measurements, and are plotted on Figure 4. The data show that the density is initially constant and then decreases (Figure 4a). However, the conductivity immediately falls rapidly with increasing particle size, particularly the grain boundary conductivity. Density or porosity clearly has a blocking effect on the transport of ions there may be other contributing factors.

Examination of the deposits with light microscopy and scanning electron microscopy showed that there was a general increase in the volume fraction of pores in the YSZ deposits with increasing particle size (Figure 5). In order to gain an insight into the mechanism of the formation of the deposits and its effect on density, wipe tests were undertaken in which glass slides were plasma sprayed using an extremely rapid gun traverse speed. This results in the deposition of isolated on the slide and enables the extent of flow of individual particles on impact with the substrate to be observed. Figure 6(a) shows that the

Table 1. Density, intragrain and grain boundary conductivities of plasma sprayed samples.

Sample	Particle size (μm)	Density (Mg / m^3)	Conductivity (μohm.cm)$^{-1}$	
			Intragrain	Grain boundary
A	20-38	5.27	63.4	141.0
B	38-52	5.30	30.3	27.7
C	52-75	5.05	20.7	7.38
D	75-90	4.64	10.9	3.79
E	90-110	4.07	9.44	3.45
M	20-110	5.18	23.7	25.8

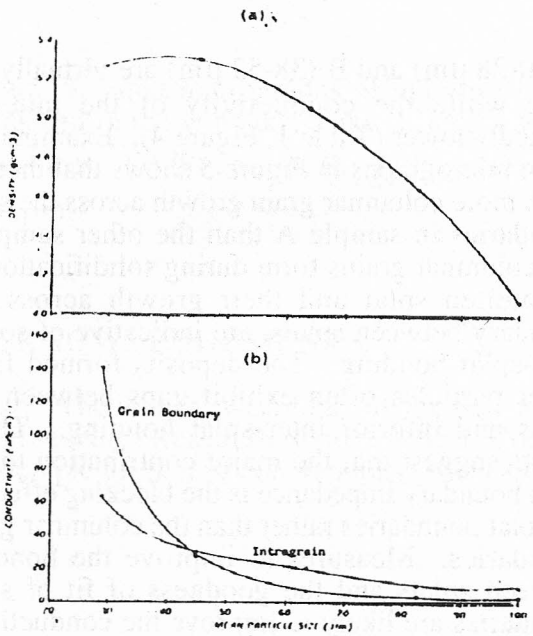

Figure 4. The effect of feed particle size on (a) density and (b) conductivity of plasma sprayed YSZ deposits.

smallest particle size produces uniformly thin, equiaxed splats indicative of extensive flow; the larger particle size in Figure 6(b) produces a much thicker splat that has undergone only limited flow, while the largest particle in Figure 6(c) appears to exhibit solid state fracture and shows little evidence of flow. The greatly reduced flow of the large particles is attributed to their lower interior temperatures in the plasma jet due to heat transfer effects. The temperature of the interior of small particles, however, rises well above their melting point and the resulting low viscosity results in extensive flow on impact and allows the mobile liquid splat to run into the contours of the underlying and surrounding splats to give a high density/low porosity deposit. The above observations were supported by X-ray diffractometry. The initial feed powder showed two monolithic peaks on either side of a larger central peak (Figure 7a) due to a heterogeneous structure and lack of stabilization of the zirconia in regions of low yttria content. Complete melting of

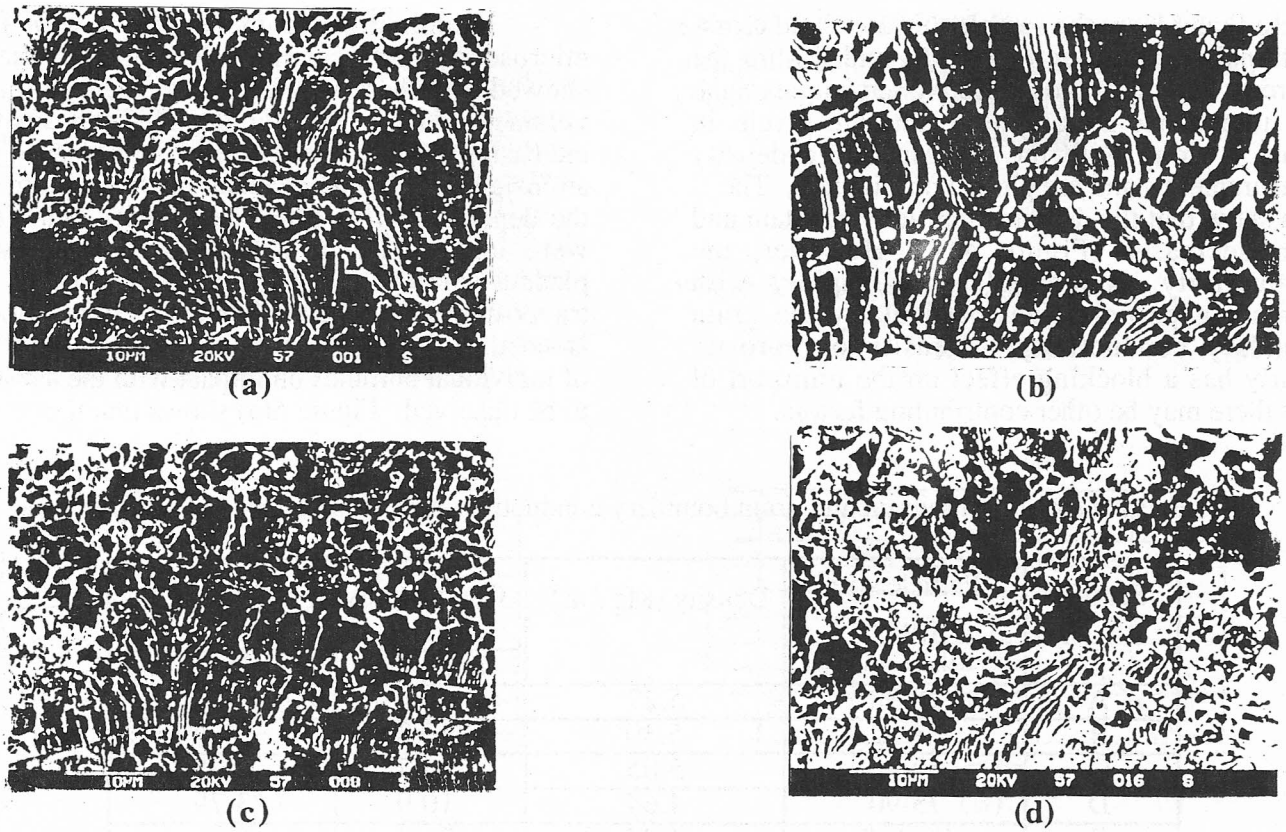

Figure 5. SEM of YSZ deposits plasma spayed with different particle sizes (a) 20-38 µm, (b) 20-38 µm, (c) 52-75 µm, (d) 90-110 µm.

a particle in the plasma provides homogenization and absence of monolithic phase on solidification, whereas some monoclinic will clearly remain after incomplete melting. The presence of a significant fraction of monoclinic phase in the deposit sprayed with the large (90-110 µm) feed particles (Figure 7b) therefore indicates incomplete melting, while virtually complete melting has occurred using the small (20-38 µm) particle size (Figure 7c). The influence of feed particle size on deposit density (Figure 4a) can thus be understood in terms of thermal diffusion distances in the plasma and particle flow on impact.

The deterioration in conductivity with increasing particle size can be attributed in part to the associated decreasing density, since pores will present a substantial blocking effect on the transport of ions through the grains and at grain boundaries. Nevertheless, the density of samples A (20-38 µm) and B (38-52 µm) are virtually the same while the conductivity of the latter is markedly lower (Table 1, Figure 4). Examination of the micrographs in Figure 5 shows that there is much more columnar grain growth across the splat boundaries in sample A than the other samples. The columnar grains form during solidification of the molten splat and their growth across the boundary between splats, are indicative of sound inter-splat bonding. The deposits formed from larger particles often exhibit gaps between the splats and inferior inter-splat bonding. These results suggest that the major contribution to the grain boundary impedance is the blocking effect of the splat boundaries rather than the columnar grain boundaries. Measures to improve the bonding between splats and the goodness of fit of splat boundaries are likely to improve the conductivity od the deposits.

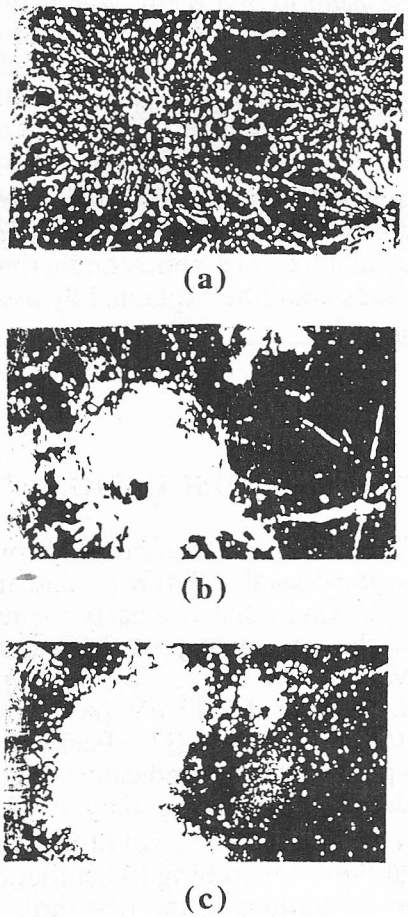

Figure 6. Light micrographs of individual splats produced in the wipe test using different particle feed sizes: (a) 20-38 μm, (b) 75-90 μm, (c) 90-110 μm.

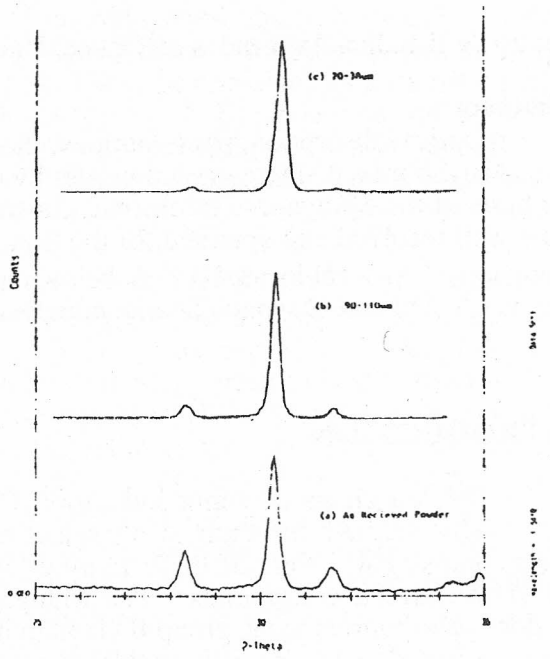

Figure 7. X-ray diffractometer traces of (a) initial feed powder (b) deposit Sprayed will 90-110 μm particles and (c) deposit sprayed with 20-38 μm feed particles.

ACKNOWLEDGEMENTS.

The authors wish to thank the Science and Engineering Research Council and Cookson Group plc for permission to publish this paper.

REFERENCES

1. A. O. Isenberg, Proc. Symp. "Electrode Materials and Processes for Energy Conversion and Storage", Electrochemical Society, 1977, 77-6, p 572.
2. G. Chiodelli, A. Magistris, M. Scagliotti and Parmigiani, J. Mater. Sci., 23 (1988) 1159.

3. J. A. Kilner and B. C. H. Steele, in "Non-Stoichiometric Oxides", Editor O. T. Sorensen, Academic Press, London 1981, p 223.